Eur. Phys. J. B **3**, 437–446 (1998)

THE EUROPEAN PHYSICAL JOURNAL B

Electronic structure and magnetism in 4d-transition metal clusters

R. Guirado-López[1], D. Spanjaard[1,a], M.-C. Desjonquères[2], and A.M. Oleś[2,b]

[1] Laboratoire de Physique des Solides, Université Paris-Sud, Bâtiment 510, 91405 Orsay, France
[2] Service de Recherche sur les Surfaces et l'Irradiation de la Matière, CE-Saclay, 91191 Gif-sur-Yvette, France

Received: 20 November 1997 / Received in final form: 9 March 1998 / Accepted: 30 March 1998

Abstract. We analyze the stability of magnetic states obtained within the tight-binding model for cubooctahedral (O_h) and icosahedral (I_h) clusters of early 4*d* (Y, Zr, Nb, Mo, and Tc) transition metals. Several metastable magnetic clusters are identified which suggests the existence of multiple magnetic solutions in realistic systems. A bulk-like parabolic behavior is observed for the binding energy of O_h and I_h clusters as a function of the atomic number along the 4*d*-series. The charge transfer on the central atom changes sign, while the average magnetic moments present an oscillatory behavior as a function of the number of *d* electrons in the cluster. Our results are in agreement with other theoretical calculations.

PACS. 36.40.Cg Electronic and magnetic properties of clusters – 71.24.+q Electronic structure of clusters and nanoparticles

1 Introduction

Recently a few new approaches were proposed to study the microscopic origin of itinerant magnetism. The simplest model of nondegenerate *s*-band gives ferromagnetic states only for very strong on-site Coulomb interaction U, unless either special conditions are satisfied by the band structure [1], or intersite matrix elements of Coulomb interactions, such as exchange, are included [2,3]. This problem becomes particularly interesting in small clusters, where the electrons are more localized than in the bulk. Therefore, the magnetic states are more likely, and studying them provides a unique opportunity of investigating the relation between cluster structure and itinerant magnetism [4,5]. The studies performed using a *s*-band model with electron correlations indicate that the magnetization exhibits shell-like oscillations [5], reflecting particular instability of open-shell configurations towards magnetic solutions. This understanding of the reasons of magnetism in clusters described by the simplest *s*-band Hubbard model provides a good starting point to analyze the situation in transition metal clusters. Knowing that the electronic-shell-like oscillations occur in the nondegenerate band model, one has to include band degeneracy in order to describe such phenomena in a realistic electronic structure. In addition, the magnetic instabilities are expected to occur more easily in degenerate bands due to the presence of intra-atomic (Hund's rule) exchange J [6].

In recent years, the transition metal clusters have been the subject of several experimental and theoretical studies. The clusters of the late 3*d* transition metals are ferromagnetic, as expected, since the tendency towards magnetism is stronger in the clusters than in the bulk. As the late 4*d* transition metals are not far from the ferromagnetic instability, the major experimental efforts have been concentrated recently on the magnetic properties of the corresponding clusters: Ru, Rh, and Pd. The quantitative prediction of magnetic states in Ru_{13}, Rh_{13}, and Pd_{13} clusters by the theoretical calculations performed within the density functional formalism [7] were confirmed by the discovery of magnetism in Rh_{13} clusters [8], and weak magnetism in Ru_{13} and Pd_{13} [9].

It may be expected that magnetic states are more difficult to realize in the clusters of earlier 4*d*-transition metals. So far, there are only a few studies which addressed this problem. Goodwin and Salahub [10] studied the stable geometries and ground-state multiplicities of small Nb_N ($N = 2 - 7$) clusters. Zhao *et al.* [11] predicted that the critical size for the magnetic-non-magnetic transition is small for Zr, Nb, Mo, and Tc clusters, but as large as $N = 93$ for Y clusters using a tight-binding Friedel model of the *d*-band and Stoner criterion. Kaiming *et al.* [12] by means of the discrete-variational local-spin-density-functional (DV-LSD) method, have studied 13-atom clusters of Y, Zr, Nb, Mo, and Tc, assuming three geometries: O_h (cubooctahedron), I_h (icosahedron), and D_{3h} (compact portion of a *hcp* lattice). The ground states of Zr_{13} and Nb_{13} were shown to correspond to the I_h structure and for Mo_{13}, Tc_{13}, and Y_{13}, the O_h cluster

[a] e-mail: spanjard@lps.u-psud.fr
[b] *Permanent address:* Institute of Physics, Jagellonian University, Reymonta 4, 30059 Kraków, Poland.

was the most stable. In the case of Y_{13}, the binding energies for the three structures were almost the same (to within 0.03 eV/at) while, on the contrary, large differences were found for the total magnetic moment M: $3\mu_B$ for the O_h and D_{3h} symmetries and a giant value of $13\mu_B$ for I_h. Zhang *et al.* [13] have performed *ab-initio* calculations for 6-atom clusters from Y to Cd. Almost all the clusters presented a non-zero average magnetic moment due to the large density of states around the Fermi level, Ru_6 and Rh_6 having the largest one. For elements of the first half of the series, all the clusters were magnetic except for Y_6. When compared with the calculation of Kaiming *et al.* for Y_{13}, this result could indicate a non-monotonic decrease of the average magnetic moment with cluster size, as found for Rh_N clusters [9]. All these results reveal that further theoretical calculations and experiments are needed in order to understand the systematic trends within the magnetic properties of $4d$ clusters.

Apart from *ab-initio* calculations, semi-empirical studies, that allow variation of the interaction parameters, may be useful to understand the trends of the magnetic and structural cluster properties. In this paper, we analyze the electronic and magnetic properties of $4d$-transition metal clusters as a function of the intra-atomic exchange J, by means of a tight-binding Hubbard Hamiltonian [14], with electron-electron interactions treated in the Hartree-Fock Approximation (HFA). Limiting ourselves to 13-atom clusters, we minimize the energy for cubooctahedral (O_h) and icosahedral (I_h) configurations to determine whether magnetism influences their relative stability. In particular, we will establish the relation between the magnetic states found and the open (closed) shell electronic configurations existing in the clusters. The results will be compared with recent *ab-initio* calculations.

The paper is organized as follows. The model Hamiltonian and the used parametrization are briefly described in Section 2. In Section 3 we present our numerical results for the magnetic states of the O_h and I_h clusters of Y, Zr, Nb, Mo, and Tc. Finally, summary and conclusions are given in Section 4.

2 The model

The semi-empirical model used here has been described in detail elsewhere [14], thus we only summarize its main points and discuss the choice of parameters. We use a tight-binding Hubbard Hamiltonian for the d band in the rotationally invariant form in orbital space [6], expressed in the basis of real d orbitals of symmetry t_{2g} (xy, yz, zx) and e_g (x^2-y^2, $3z^2-r^2$). In this basis the most important matrix elements of the on-site Coulomb interaction, *i.e.*, involving one or two orbitals are: intra-orbital ($U+2J$) and inter-orbital (U) Coulomb and exchange (J) integrals.

Note that strictly speaking there are also a very limited number of non-vanishing matrix elements of the on-site Coulomb interaction involving three or even four orbitals [15]. However, such matrix elements are small due to the angular dependence of atomic d orbitals pointing along different directions of space. Therefore, we neglect these interaction elements in what follows, as usually done in this field. Similarly, all inter-orbital Coulomb and exchange integrals are not rigorously equal. They have been replaced by their average value. This approximation is expected to be valid when the d electrons are roughly equally distributed between the five d orbitals at each site. We will see in the following that this approximation is fully justified.

Finally, the Coulomb interaction between sites i and j, V_{ij}, is also introduced. The electronic structure of the cluster is determined by solving this model with the interactions treated in the HFA. Using the basis of $4d$ atomic spin-orbitals $|i\lambda\sigma\rangle$ centered at each site i, one finds [14]

$$H_{HFA} = \sum_{i\lambda,\sigma} \epsilon_{i\lambda\sigma} n_{i\lambda\sigma} + \sum_{i,\lambda,\mu\neq\lambda,\sigma} h_{i,\lambda\mu,\sigma} a^\dagger_{i\lambda\sigma} a_{i\mu\sigma} + \sum_{i\lambda,j\mu,i\neq j,\sigma} t_{i\lambda,j\mu} a^\dagger_{i\lambda\sigma} a_{j\mu\sigma} \quad (1)$$

in the usual notation. The on-site energy levels, $\epsilon_{i\lambda\sigma}$, are functions of the spin-orbital occupation numbers $\langle n_{i\lambda\sigma}\rangle$ and electron-electron interactions. For convenience we measure them from the average value ϵ^0_d, obtained when each atom is occupied by N_a electrons ($N_a = N_e/13$, where N_e is the total number of electrons in the cluster) and each individual orbital by $n_a = N_a/5$ electrons. This gives

$$\epsilon_{i\lambda\sigma} = \epsilon^o_d + (U - \frac{1}{2}J)(N_i - N_a) - \frac{1}{2}(U-3J)(\langle n_{i\lambda}\rangle - n_a) - \frac{1}{2}\xi_\sigma J M_i - \frac{1}{2}\xi_\sigma (U+J)\langle m_{i\lambda}\rangle + \sum_{j(i)} V_{ij}(N_j - N_a), \quad (2)$$

where $\xi_\sigma = \pm 1$ for $\sigma = \uparrow,\downarrow$, and $j(i)$ stands for the neighbors of site i. Here we have introduced the orbital occupation number $\langle n_{i\lambda}\rangle = \langle n_{i\lambda\uparrow}\rangle + \langle n_{i\lambda\downarrow}\rangle$, and the orbital magnetic moment $\langle m_{i\lambda}\rangle = \langle n_{i\lambda\uparrow}\rangle - \langle n_{i\lambda\downarrow}\rangle$. N_i is the total number of electrons at atom i, and M_i is the magnetic moment. The quantity V_{ij} stands for the intersite Coulomb interaction assumed to be inversely proportional to the bond length R_{ij}. In the bulk $N_j = N_a$ and the last term in equation (2) vanishes. The way of calculating the effective levels is thus comparable to that used in LDA+U approach [16].

The second term in equation (1) corresponds to the intrasite inter-orbital Fock terms ($\bar\sigma = -\sigma$),

$$h_{i,\lambda\mu,\sigma} = (J-U)\langle a^\dagger_{i\mu,\sigma} a_{i\lambda,\sigma}\rangle + 2J\langle a^\dagger_{i\mu,\bar\sigma} a_{i\lambda,\bar\sigma}\rangle. \quad (3)$$

They vanish in the bulk since $\langle a^\dagger_{i\lambda,\sigma} a_{i\mu,\sigma}\rangle = 0$, if $\lambda \neq \mu$ due to cubic symmetry. This is, however, not the case when the symmetry is lowered and these terms have to be included in order to conserve the actual symmetry properties of the system [14]. Finally the hopping integrals $t_{i\lambda,j\mu}$ are obtained in the Slater-Koster scheme [17] from the parameters ($dd\sigma$), ($dd\pi$) and ($dd\delta$). They are assumed to

Table 1. Hopping parameter at equilibrium bulk distance, $(dd\sigma)_0$, and local electron-electron interaction parameters: U and J (all in eV) estimated for the early 4*d* transition metals.

	$(dd\sigma)_0$	U	J
Y	−0.7875	0.80	0.30
Zr	−0.9250	0.90	0.34
Nb	−0.9875	1.15	0.38
Mo	−1.0250	1.10	0.41
Tc	−0.9875	1.15	0.45

Table 2. Electronic filling N_e for each cluster, equilibrium distance R_0 (Å), bulk cohesive energy E_{coh} (eV/at), bulk modulus B (eV/at) and the parameters of the repulsive potential, A_0 (eV) and pR_0, for the early 4*d* transition metals.

	N_e	R_0	E_{coh}	B	A_0	pR_0
Y	26	3.600	4.24	7.55	0.232	6.93
Zr	40	3.252	6.33	12.46	0.359	7.29
Nb	56	2.857	7.58	19.14	0.447	8.25
Mo	68	2.728	6.83	26.54	0.472	10.24
Tc	82	2.786	6.60	26.04	0.414	10.31

vanish beyond first nearest neighbors and to decrease exponentially with a damping exponent q ($\sim \exp(-qR_{ij})$) when the distance R_{ij} increases. We have adopted the relations $(dd\pi) = -(dd\sigma)/2$ and $(dd\delta) = 0$, and the values of $(dd\sigma)$ at the bulk interatomic spacing R_o have been fitted to the bandwidths of the bulk transition metals. They are given in Table 1 as $(dd\sigma)_o$.

The bond length and the magnetic state of the clusters are determined by minimizing the total energy,

$$E = \langle H_{HFA} \rangle - \langle H_{int,HFA} \rangle + E_{rep}. \quad (4)$$

The first term is the sum of the occupied one-particle energies in the HFA, while the second term is the correction for the double counting. The repulsive energy E_{rep} is described by a sum of pair interaction energies $A(R_{ij})$ between first nearest neighbors. The function $A(R_{ij}) = A_0 \exp(-pR_{ij})$ is of the Born-Mayer type, *i.e.*, decreases exponentially with increasing bond length.

We use the ratio $p/q = 3$ which fits [18] the universal potential energy curves of Smith *et al.* [19]. The value of pR_0 is then deduced for each element from the experimental ratio of the bulk modulus B to the cohesive energy E_{coh}, as given in Table 2. It is well known that both quantities are underestimated in a pure *d*-band model but their ratio should be correctly reproduced. Finally, the value of the repulsive pair energy A_0 at $R_{ij} = R_0$ (given in Tab. 2) is deduced from the equilibrium equation for the bulk.

The on-site interactions U have been estimated by Van der Marel and Sawatzky [20] using spectroscopic data. We use these values for the considered transition metal clusters, but as our approach does not treat explicitly the correlation effects, we have screened them to simulate the effects of electron correlations. The resulting values of U adopted in the calculations are given in Table 1. The values of the exchange interaction J, given in Table 1, are determined as a function of the atomic number using an empirical formula found in reference [20]. The intersite Coulomb interaction at the bulk distance $R_{ij} = R_0$ is set equal to 0.5 eV for all considered clusters [14]. This parameter has an indirect influence on the magnetism since it plays a role in the magnitude of the charge transfer between the atoms placed in nonequivalent positions of the considered cluster. It is not very precisely known, however the chosen value has a reasonable order of magnitude and it has been shown [14] that the total moment of the cluster is unchanged when V is varied from 0.3 to at least 0.6 eV.

3 Results and discussion

The exchange integral J plays a decisive role in magnetism of transition metals, but it is not known accurately enough. Thus, in order to study the appearance of magnetism in 13-atom 4*d*-transition metal clusters in a systematic way, we calculate the ground state and its magnetization as a function of the exchange interaction, using the values $0 \leq J \leq 0.6$ eV which cover the physically interesting range. Within our model, we explore also the existence of multiple magnetic solutions by changing our initial spin-polarized electronic configuration in our self-consistent diagonalization process. The former procedure could be equivalent to different choices of the input potential in Local Spin Density (LSD) calculations. These multiple magnetic solutions correspond to local minima of the total energy as a function of the magnetic moment of the system of a given geometry, among which the one that gives the lowest total energy is regarded as the ground state of the cluster and the rest with higher energies are only metastable states.

3.1 Qualitative trends

The number of electrons in the Highest Occupied Molecular Orbital (HOMO) of a cluster plays a significant role in determining its ground-state electronic properties and the structural stability. Clusters with a fully occupied HOMO have a ground state which has a closed electronic shell. This type of configuration is expected to be quite stable as has been shown in the previous calculations [14]. In contrast, for a cluster with an unfilled HOMO, the ground state has an open electronic shell, being highly degenerate and as a consequence, easier to destabilize by the increase of the electronic interactions or by modifications in the interatomic distance.

Consider first nonmagnetic clusters without electron-electron interactions ($U = V = J = 0$), with the energy levels shown in Figure 1 for the cubooctahedral and icosahedral clusters treated in this work. We have chosen realistic numbers of *d* electrons N_e for 4*d* clusters as given in Table 2. These values are even since we want to concentrate ourselves on the nontrivial magnetic instabilities promoted by electron-electron interactions. One finds that the O_h Y_{13}, Nb_{13} and I_h Tc_{13}, are closed shell systems, while the O_h Zr_{13}, Mo_{13} and Tc_{13} and I_h Y_{13}, Zr_{13}, Nb_{13}

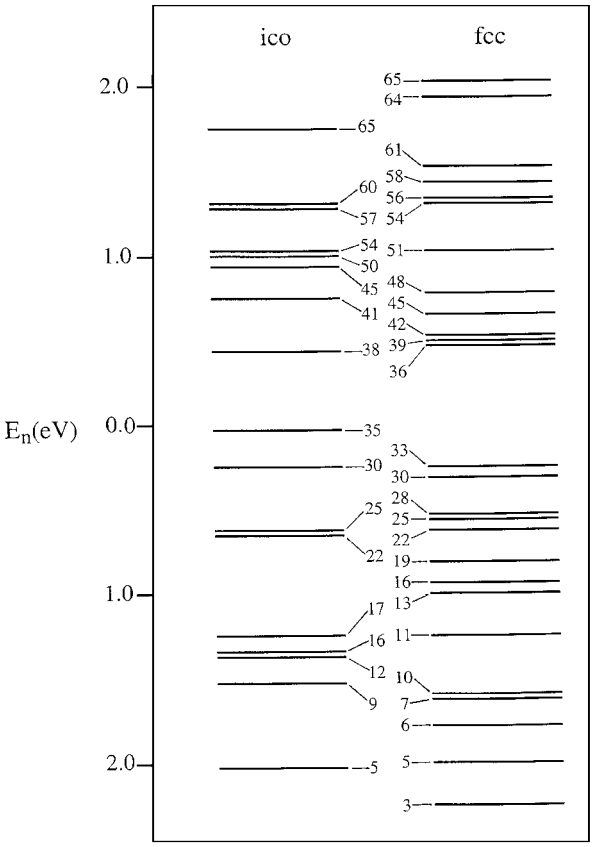

Fig. 1. Tight-binding electronic structure for icosahedral (ico) and cubo-octahedral (fcc) 13-atom transition metal clusters as obtained with the parameters of Zr: $(dd\sigma) = -0.9250$, $(dd\pi) = -(dd\sigma)/2$, and $(dd\delta) = 0$ (in eV), in the absence of interactions ($U = J = V = 0$). The total number of electrons corresponding to a closed shell configuration for one spin direction is indicated. These numbers are the same for other elements since the corresponding energies can be obtained by a simple scaling.

and Mo_{13} are open shell structures. As a result, the instability towards magnetic solutions (if any) is expected to occur at smaller values of J for open shell than for closed shell structures, and particular magnetizations M which correspond to the closed shell systems are expected to be more stable than the others.

The numerical results for the magnetization M as a function of the exchange integral J obtained for Y, Zr, Nb, Mo, and Tc are presented in Figures 2–6, using the values of U given in Table 1, and the electron filling and the repulsive potential parameters given in Table 2. An energy minimization was performed for each value of J, and the existence of multiple self-consistent solutions was analyzed by using different initial conditions for the self-consistent procedure. These metastable solutions correspond to different values of magnetization and to different bond lengths; they are shown in Figures 2–6 by different symbols.

We note that, following a general tendency in 13-atom transition metal clusters, the icosahedron is more stable

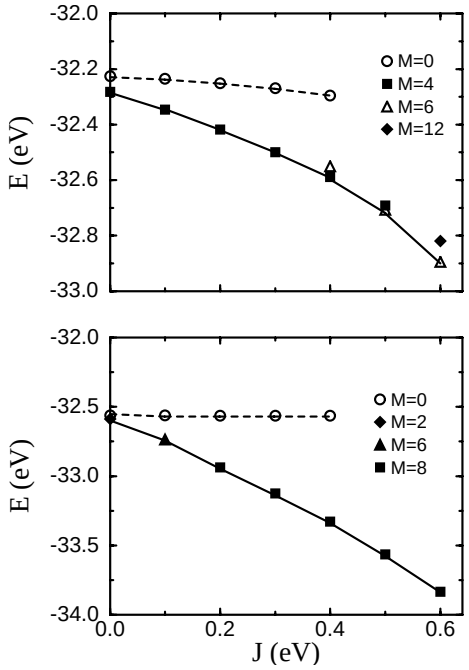

Fig. 2. Total binding energy E for Y_{13} clusters as a function of Hund's rule exchange J, calculated for cubooctahedral (top) and icosahedral (bottom) configurations. The points stand for the self-consistently found solutions (with J increasing by steps of 0.1 eV) with different total magnetizations, while the full and dashed lines are guides to the eye to indicate the ground state and the nonmagnetic state, respectively.

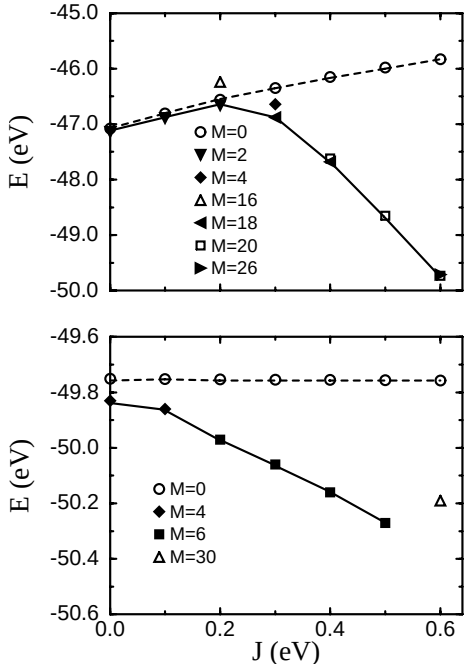

Fig. 3. Same caption as Figure 2 for Zr_{13} clusters.

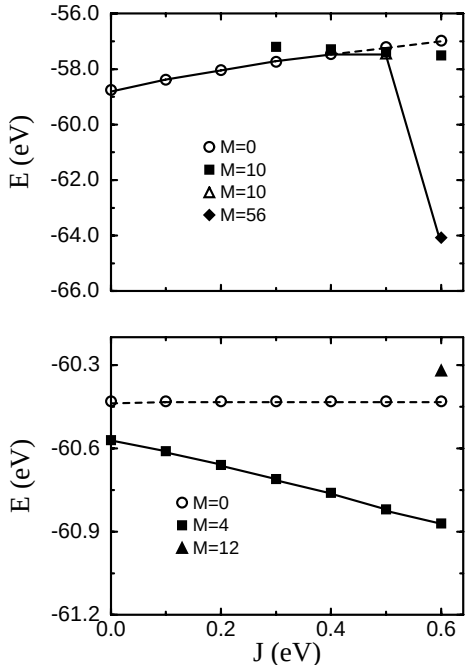

Fig. 4. Same caption as Figure 2 for Nb_{13} clusters.

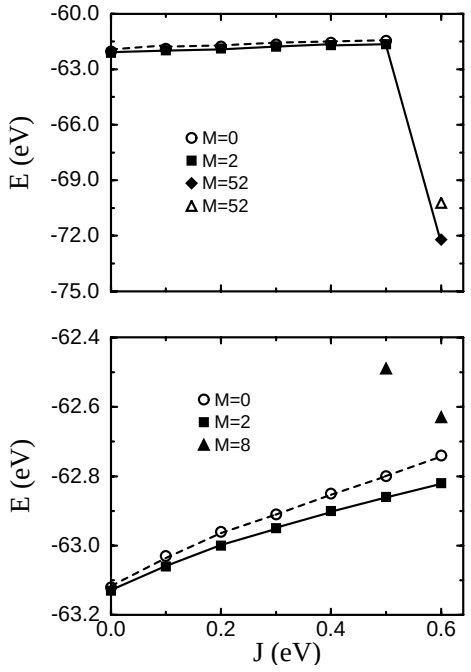

Fig. 5. Same caption as Figure 2 for Mo_{13} clusters.

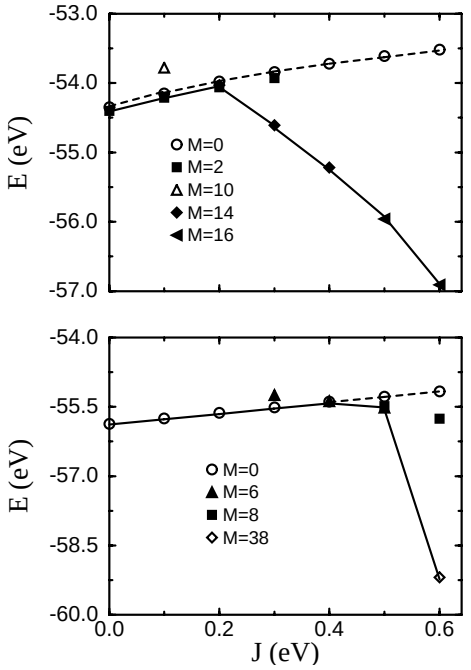

Fig. 6. Same caption as Figure 2 for Tc_{13} clusters.

than the cubooctahedron for small values of J in all cases. However, the O_h structure becomes energetically favored for Nb_{13} and Mo_{13} (Figs. 4 and 5) when J is large due to the existence of states with a high value of M.

3.2 Non-magnetic states

The non-magnetic states were obtained for all the aggregates, as seen in Figures 2–6. We observe that in most cases, the energy of the non-magnetic states increases with increasing J, which means that the electron interaction energy cannot be lowered by changes in the charge distribution alone. Nevertheless, in I_h Y_{13}, Zr_{13} and Nb_{13}, the total binding energy E is almost independent of J while for O_h Y_{13} it decreases slightly. In this last case the cluster has a closed shell structure for which the molecular orbitals are not strongly modified by changes in the electronic interactions and, as a consequence, the total energy E is almost independent of J. For I_h Y_{13}, Zr_{13} and Nb_{13}, which are open-shell structures, such a constant behavior could be due to the assumption of a uniform relaxation which is not allowing the 13-atom cluster to perform more complicated distortions that might lower the symmetry of the structure and also its total energy.

For O_h and I_h Y_{13}, the non-magnetic states could not be obtained for $J > 0.4$ eV and in O_h Mo_{13} for $J = 0.6$ eV. In the remaining clusters this solution was present for all the considered values of the exchange parameter in both types of symmetries. Note that in Nb_{13}, the magnetic solutions are obtained already at J =0 for I_h, whereas for the O_h cluster a value of J larger than 0.3 eV is needed. Actually, the I_h Nb_{13} cluster is an open shell structure and thus easier to destabilize by increasing exchange interactions, while the cubooctahedral cluster is a closed shell system and thus more robust. This behavior is reversed for the Tc_{13} cluster, in which for the I_h symmetry (closed shell), a value of $J = 0.3$ eV was required to stabilize the magnetic solution, while in the O_h symmetry (open shell) for $J = 0$ eV, we have already a value of 2 for the total magnetization.

3.3 Magnetic states

In general, we can see that increasing the exchange interaction J results in the appearance of magnetic states with larger values of the total magnetization. Typically a few discrete values of the magnetization are realized which correspond to closed shell configurations for at least one spin direction, and the energy of the cluster is decreased. However, in Mo_{13} we observe an inverse behavior – increasing the value of exchange interaction increases the energy of the cluster. For sufficiently large values of J solutions with larger magnetizations appear, and the total energy begins to decrease. Note that contrary to the O_h structure, in the I_h Mo_{13} cluster, this high-spin solution has a smaller binding energy, which indicates that for this cluster, the tendency to lower magnetization is preferred.

In almost all the clusters, the magnetic states were found already at $J = 0$ eV, which shows a strong tendency towards magnetism. Augmenting the exchange parameter results in an increase of the splitting between the molecular orbitals for up- and down-spins, thus producing large changes in the magnetization of the system, as one can see for example in Figure 3 (top) for values of J larger than 0.2 eV. In all the clusters, with the exception of O_h Nb_{13}, a value of $J = 0.6$ eV, was not enough to reach the fully polarized saturated state. However, with the variation of the exchange parameter, we can see the existence of several intermediate solutions for the total magnetization M in all our aggregates. These states have an antiferromagnetic (AF) or ferromagnetic (FM) ordering of the magnetic moment on the central atom relative to that of the surface atoms.

For Y_{13} (Fig. 2) one notes that only low-spin states are realized since when J increases from 0 to 0.6 eV, the ground state magnetization increases from $M = 4$ to $M = 6$ in the O_h structure and from $M = 2$ to $M = 8$ in the I_h structure. For both clusters, all these low-spin states present an AF configuration.

In the I_h Zr_{13} cluster (Fig. 3) the ground state evolves from a FM configuration ($M = 4$) to an AF one with $M = 6$ and 30 successively. The O_h Zr_{13} cluster presents a more abundant magnetic structure. When J increases one finds ground states with M =2 (AF), 18 (FM), 20 (FM) and 26 (AF).

For Nb_{13} (Fig. 4) the ground state in the I_h structure is AF with $M = 4$ for any value of J. In the O_h symmetry it is magnetic only when $J = 0.5$ eV ($M = 10$ (AF)) and reaches the FM saturation state ($M = 56$) at $J = 0.6$ eV. Note that for $J = 0.5$ eV a second (FM) solution with $M = 10$ is also obtained, but it is slightly less stable than the AF one with the same value of M.

In Mo_{13} for the I_h cluster (Fig. 5), the ground state is FM with $M = 2$ for all the values of J. For O_h clusters it is AF with $M = 2$, and its magnetization changes abruptly to $M = 52$ when $J = 0.6$ eV. Note that for this last value of J another (but less stable) AF solution was also found with $M = 52$, corresponding to a different spin spatial distribution.

Finally, in the Tc_{13} clusters (Fig. 6) one finds a more abundant magnetic structure. Magnetic ground states are stable for the I_h cluster at $J > 0.3$ eV, with first $M = 6$ and then $M = 38$; both states being AF. For the O_h symmetry, we find $M = 2$ for $J \leq 0.2$ eV, and $M = 14$ and 16 at higher values of J, all of them with AF configurations. In this case, similarly to the Y_{13} cluster, it seems that the trend towards AF order is also independent of the cluster structure.

Table 3. The calculated equilibrium bond lengths (Å), average energies $\langle E \rangle$ (eV/at) and average magnetic moment $\langle M \rangle$ (μ_B/at) per atom for each cluster. For comparison the results for $\langle M_{LSD} \rangle$ obtained in reference [12] are also shown. The ground state for each geometry is indicated by the superscript ($*$).

cluster	symmetry	r	$\langle E \rangle$	$\langle M \rangle$	$\langle M_{LSD} \rangle$
Y_{13}	O_h^*	3.253	2.500	0.30	0.23
	O_h	3.255	2.481	0.00	
	I_h^*	3.215	2.547	0.61	1.00
	I_h	3.210	2.505	0.00	
Zr_{13}	O_h^*	3.033	3.630	1.38	0.00
	O_h	2.998	3.569	0.30	
	O_h	2.993	3.559	0.00	
	I_h^*	2.990	3.853	0.46	0.30
	I_h	2.980	3.826	0.00	
Nb_{13}	O_h^*	2.657	4.424	0.00	0.07
	O_h	2.665	4.405	0.77	
	I_h^*	2.590	4.673	0.30	0.53
	I_h	2.588	4.650	0.00	
Mo_{13}	O_h^*	2.568	4.746	0.15	0.15
	O_h	2.567	4.734	0.00	
	I_h^*	2.515	4.837	0.15	0.00
	I_h	2.515	4.833	0.00	
Tc_{13}	O_h^*	2.638	4.272	1.07	0.07
	O_h	2.645	4.270	1.23	
	O_h	2.622	4.127	0.00	
	I_h^*	2.570	4.265	0.46	1.00
	I_h	2.568	4.256	0.00	

By analyzing the stable and metastable magnetic states found in the considered clusters one finds that, save for the solution $M = 52$ of O_h Mo_{13}, the population of at least one spin direction corresponds to a closed shell structure in absence of interactions ($U = J = V = 0$, Fig. 1). However, when these interactions are present they very often lead to level crossings since the atomic levels of the central atom and the outside ones are no longer equal and may become rather different, especially when there are large charge transfers or/and large local magnetic moments with AF ordering. These level crossings may lead to modifications of the electronic populations (number of electrons with spin up $N_\uparrow$ or spin down $N_\downarrow$) corresponding to closed shells. This is actually the case for O_h Mo_{13} and $M = 52$ for which the spin up configuration ($N_\uparrow = 60$) becomes closed shell in the presence of interactions. We have verified that for all other cases, even though level

Table 4. Local electronic fillings and local magnetic moments (in units of μ_B/at) calculated for the central (N_0 and M_0) and the outside (N_i and M_i) atoms in the ground states of 13-atom transition metal clusters of two symmetries: O_h and I_h. The data for Ru_{13}, Rh_{13}, and Pd_{13} were taken from reference [14]. Average moments per cluster atom $\langle M \rangle$ (μ_B/at) are given in the last column.

cluster	symmetry	N_0	N_i	M_0	M_i	$\langle M \rangle$
Y_{13}	O_h	3.97	1.83	−0.15	0.34	0.30
	I_h	4.41	1.80	−0.32	0.69	0.61
Zr_{13}	O_h	4.22	2.98	0.34	1.47	1.38
	I_h	3.99	3.00	−0.07	0.50	0.46
Nb_{13}	O_h	4.61	4.28	0.00	0.00	0.00
	I_h	4.26	4.31	−0.23	0.35	0.30
Mo_{13}	O_h	5.29	5.22	−0.28	0.19	0.15
	I_h	5.13	5.23	0.29	0.14	0.15
Tc_{13}	O_h	5.48	6.37	−1.08	1.25	1.07
	I_h	5.50	6.37	−0.77	0.56	0.46
Ru_{13}	O_h	5.48	7.38	−2.13	2.18	1.85
	I_h	5.52	7.37	−2.21	2.18	1.85
Rh_{13}	O_h	6.59	8.45	0.66	1.11	1.08
	I_h	7.45	8.38	2.55	1.62	1.69
Pd_{13}	O_h	7.32	9.56	2.68	0.44	0.62
	I_h	7.35	9.55	2.65	0.45	0.62

crossings may occur, the population of at least one spin direction still corresponds to a closed shell structure.

In general, we can say that the cubooctahedral clusters are richer in magnetic structure due to their lower degeneracies of the electronic levels (see Fig. 1). Moreover, the AF orientation of the moment on the central atom with respect to the outside shell is preferred in most of the clusters. This tendency to antiferromagnetism in our aggregates, is due to the fact that the charge distribution within the structures, results in values close to half-filling (as we can see in Tab. 4 for the realistic values of J) for the electronic occupation in the central atom. As a result, the magnetic moments which are formed in the center are antiferromagnetically aligned with respect to the outside shell, following the general tendency towards AF order for a half-filled d-band.

The distribution of charge and magnetic moments within the structures turns out to be very inhomogeneous (*i.e.*, large differences between the central and surface atoms) for some of the clusters when varying J. This inhomogeneity is particularly large at the beginning of the series, and also at the end of the series, as already shown in previous calculations [14]. In almost all our aggregates, and for intermediate values of J, the low-spin magnetic solutions have a local magnetic moment larger in the surface than in the central atom. This is a consequence of the reduced coordination number in the atoms of the outside shell which enhances the electron localization and promotes the transitions towards magnetic states.

3.4 Ground state properties

In Table 3 we present the calculated magnetic ground states in Y, Zr, Nb, Mo, and Tc clusters, as obtained for our realistic parameters presented in Tables 1 and 2. As usual, we obtain bond length contractions for all clusters as compared with their respective bulk interatomic spacing. The largest contraction is equal to 10.6%, for Y in the I_h symmetry and the smallest one amounts to 5.3% for Tc in the cubooctahedral structure. The binding energy $\langle E \rangle$ per atom for each kind of cluster is smaller than its bulk binding energy (see Tab. 2), and it increases with atomic number as we move from Y to Mo. Obviously, due to the neglect of *sp*-electrons and *spd*-hybridization effects, our calculated binding energies are underestimated as compared to the *ab-initio* calculation of Kaiming *et al.* for the same clusters [12]. However, as we approach the middle of the series, the difference between our calculated binding energies E and the *ab-initio* results is less pronounced. In the case of Mo, our d-electron calculations are able to match almost exactly the *ab-initio* result [12] for both types of symmetries ($\langle E(O_h) \rangle = 4.77$ eV/at and $\langle E(I_h) \rangle = 4.58$ eV/at). This result is in agreement with previous calculations [22] which showed that the d-band contribution to the total energy is the dominant part for elements in the middle of the transition metal series. Note, however, that in our calculation, the I_h Mo_{13} cluster is the ground state structure.

In the case of Y_{13}, Zr_{13}, Nb_{13}, and Mo_{13}, we can see that the most stable structure is I_h, with an energy gain of 0.04, 0.22, 0.25, and 0.09 eV/at, respectively, with respect to the O_h cluster. However, for Tc_{13} the O_h symmetry corresponds to the most stable structure with an energy difference of 0.007 eV/at. These results are in agreement with a general argument stating that 13-atom transition metal clusters tend to have I_h symmetry in their ground state, because the directional bonding is not too important in metals and only in this geometry do all surface atoms have the maximum number of nearest neighbor atoms. Contradicting this general tendency, it has been found in reference [12] that O_h Mo_{13}, Tc_{13}, and Y_{13} are the most stable clusters. However, in the case of Y_{13}, the energy difference between the O_h, I_h and D_{3h} structures is less than 0.03 eV/at (a value which is of the order of the numerical accuracy), therefore it is difficult to draw a definite conclusion about the most stable cluster. In agreement with the *ab-initio* results [12], we find that the O_h symmetry corresponds to the ground state structure for the Tc_{13} cluster. Our calculated average magnetic moment for the I_h Y_{13} is large compared with the rest of the clusters (in agreement with the *ab-initio* result) while contrary to the calculation of Kaiming *et al.* [12], our largest value for M in Zr_{13} and Tc_{13} is found in the O_h symmetry. It is important to note, however, that one of the self-consistent solutions for O_h Zr_{13} and Tc_{13} clusters has a zero magnetic moment in agreement with the *ab-initio* result, although in our model these solutions correspond to metastable states.

As we can see in Table 3 (for the most stable geometrical structures), all the clusters are magnetic with the exception of O_h Nb_{13}. Comparing with the work of

Kaiming *et al.* [12], we observe that our calculated average magnetic moments per atom $\langle M \rangle$ follow the same trends as the *ab-initio* results and that they are of the same order in most cases. This result gives some support to our choice of parameters deduced from the bulk experimental quantities. At the same time, we can see also the importance of investigating a possibility of multiple magnetic solutions in transition metal clusters. Our calculations have shown that the energy differences between the ground state and the metastable structures can be very small (typically $\Delta E \approx 0.02$ eV/at, see Tab. 3), however large variations can be obtained in the magnetic properties.

The contractions in the distance obtained in our work are larger than the ones reported in reference [12]. However, it is important to emphasize that our average magnetic moments have revealed to be constant with changes in the interatomic spacing of at least up to 10% of contraction. As a consequence, our larger contractions do not affect the calculated value for $\langle M \rangle$. Contrary to the average magnetic moment, the local magnetic moments (moments in the central atom and on the surface) are sensitive to changes in the interatomic distance and in the geometry of the cluster. Our results suggest that the main effect generating magnetism in our structures can be attributed to the reduction in the coordination.

Using the calculations reported in reference [14] for Ru_{13}, Rh_{13}, and Pd_{13}, we plot in Figure 7 the binding energy E, the charge inhomogeneity,

$$\Delta N_e = N_0 - N_i, \tag{5}$$

N_0 and N_i being the number of electrons of the central and outside (surface) atoms, respectively, and the average magnetic moment per atom $\langle M \rangle$ as functions of the atomic number along the 4*d* series. We observe a parabolic dependence of the binding energy E (Fig. 7a) on the atomic number for I_h and O_h clusters. A similar behavior is also observed for the same elements in the bulk state. This result reveals that even for such small structures the *d*-band filling plays the leading role in determining the variations of binding properties along the 4*d*-series.

The charge distribution is found to be anisotropic, with large inhomogeneity ($\Delta N_e > 0$) for the elements at the beginning of the 4*d* series (Fig. 7b) especially for the I_h symmetry. Increasing the atomic number results in a more uniform charge distribution for both types of clusters ($\Delta N_e \approx 0$), as found in the case of Mo_{13} for cubooctahedral structures and in Nb_{13} for icosahedral clusters. Starting from Tc_{13}, anisotropy increases again, but the charge inhomogeneity is reversed, and the surface atoms absorb electrons from the central site ($\Delta N_e < 0$). This inversion in the fluctuation of charge, similar to that obtained on infinite surfaces [23], is due to the reduced coordination on the atoms located in the surface of the clusters, which produces a narrower density of states as compared to the one given in the bulk structure. For elements with an almost empty *d*-band the Fermi level lies at the bottom of the band; as a consequence a reduction in the band width results in a loss of electronic charge as compared to the average occupancy in the bulk. In a similar way, for elements with an almost complete *d*-band, the Fermi level is located at the top of the band, as a result a narrower band width will increase the number of electrons.

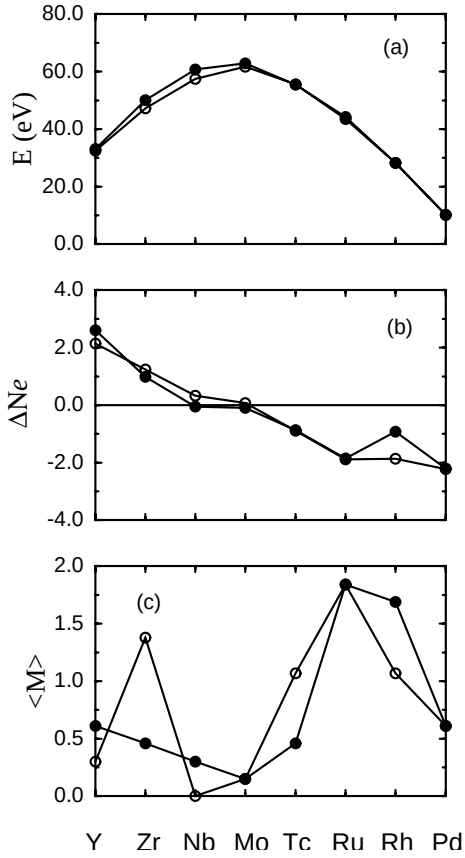

Fig. 7. The total binding energy E (eV), the charge inhomogeneity ΔN_e, and the average magnetic moment $\langle M \rangle$ (μ_B/at) as a function of the atomic number for O_h (○) and I_h (●) 13-atom 4*d*-transition metal clusters.

A characteristic non-monotonic behavior of the average magnetic moment $\langle M \rangle$ is also found as a function of electronic filling in both (O_h and I_h) structures (Fig. 7c). The magnetization first increases with increasing electron (hole) filling starting from empty (full) *d*-states, and next goes through a pronounced minimum, found for Nb in the O_h geometry and for Mo in the I_h structure, respectively. These oscillations in $\langle M \rangle$ have no bulk counterpart since none of the 4*d*-transition metals are magnetic in the bulk phase. However, similar changes of the local magnetic moment of the impurity X have been observed in I_h $Cu_{12}X$ clusters [24], when X is varied along the 4*d*-transition metal series. Calculations for bigger clusters as a function of the atomic number would allow to investigate how these oscillations evolve to the non-magnetic state. The dependence of $\langle M \rangle$ on the atomic number could also give an indication of the different magnetic-non-magnetic transitions possible in the 4*d*-transition metal clusters.

The magnetic order within the structures is shown to be antiferromagnetic for most of the clusters. Only in O_h Zr_{13} and I_h Mo_{13} a ferromagnetic solution is found. Note

that most often in our clusters, surface atoms have larger magnetic moments (see Tab. 4) since the coordination number is smaller, thus the localization of the electrons increases and enhances the magnetic properties. However, in O_h and I_h Mo_{13} and in I_h Tc_{13}, the central atom is the one with the largest magnetic moment.

Finally, we have checked on the particular case of Y_{13} the effect of replacing the inter-orbital Coulomb $U_{\lambda\mu}$ and exchange $J_{\lambda\mu}$ integrals by their average values. If this last approximation is removed, equations (2, 3) become:

$$\epsilon_{i\lambda\sigma} = \epsilon_d^o + U_{\lambda\lambda}\left(\langle n_{i\lambda\bar{\sigma}}\rangle - \frac{N_a}{10}\right) + \sum_{\mu\neq\lambda}\left[U_{\lambda\mu}\left(\langle n_{i\mu}\rangle - \frac{N_a}{5}\right) - J_{\lambda\mu}\left(\langle n_{i\mu\sigma}\rangle - \frac{N_a}{10}\right)\right], \quad (6)$$

and

$$h_{i,\lambda\mu,\sigma} = -U_{\lambda\mu}\langle a^{\dagger}_{i\mu,\sigma}a_{i\lambda,\sigma}\rangle + J_{\lambda\mu}(\langle a^{\dagger}_{i\mu,\sigma}a_{i\lambda,\sigma}\rangle + 2\langle a^{\dagger}_{i\mu,\bar{\sigma}}a_{i\lambda,\bar{\sigma}}\rangle). \quad (7)$$

The matrix elements $J_{\lambda\mu}$ are given in Table 1 of reference [25]. They are expressed as a function of two parameters: $J^{'} = (J_{e_g e_g^{'}} + J_{t_{2g}t_{2g}^{'}})/2$ and $\Delta J^{'} = J_{e_g e_g^{'}} - J_{t_{2g}t_{2g}^{'}}$. The parameter $U_{\lambda\lambda}$ is written as $U_{\lambda\lambda} = U^{'} + 2J^{'}$ which determines $U^{'}$. Then all the matrix elements $U_{\lambda\mu}$ ($\lambda \neq \mu$) are deduced from the formula: $U_{\lambda\lambda} = U_{\lambda\mu} + 2J_{\lambda\mu}$.

According to references [15,25] we have taken $\Delta J^{'} = 0.15J^{'}$ and the values of $U^{'}$ and $J^{'}$ have been chosen in such a way that the values of U and J used in our simplified Hamiltonian are the average values of the inter-orbital Coulomb and exchange integrals, *i.e.*, $U = U^{'} + 2\Delta J^{'}$ and $J = J^{'} - \Delta J^{'}$. Note that $U + 2J = U^{'} + 2J^{'}$, so that the diagonal elements $U_{\lambda\lambda}$ remain the same in both approaches.

The results for Y_{13} are given in Figure 8. The similarities with Figure 2 are striking. The main difference concerns the metastable nonmagnetic state which disappears for a smaller value of J. The calculated values of the interatomic distances and the total energy per atom in the ground state are nearly unchanged. This fully justifies the approximation made.

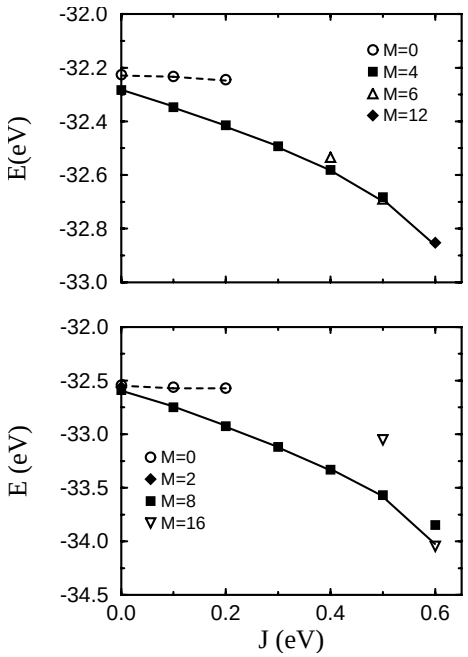

Fig. 8. Same caption as Figure 2 but the results have been obtained taking into account the anisotropy of intrasite inter-orbital Coulomb $U_{\lambda\mu}$ and exchange $J_{\lambda\mu}$ integrals.

4 Summary and conclusions

We have presented the results of self-consistent calculations for the electronic and magnetic properties of Y_{13}, Zr_{13}, Nb_{13}, Mo_{13}, and Tc_{13} clusters, using realistic tight binding parameters. They are summarized and compared with the previous calculations [14] for Ru_{13}, Rh_{13}, and Pd_{13} clusters in Table 4. All the considered clusters were found to be magnetic, with the exception of the O_h Nb_{13}. On comparing the reported results with the calculations of Kaiming *et al.* [12] we conclude that our calculated values of $\langle M\rangle$ follow the same trends as the *ab-initio* ones. The largest difference was obtained for the O_h Zr_{13} and Tc_{13} clusters, however in each of these cases one of our metastable solutions was in good agreement with the more sophisticated calculation.

Our calculated equilibrium distances were found to be smaller than in the *ab-initio* results, since the *sp*-electrons and *sp*-*d* hybridization were not explicitly included in the present model and have a net repulsive effect at the beginning of the *d* series [22]. However, it was found that the average magnetic moments were constant over a large range of changes in the interatomic distance (10%), a feature which gives some support to our calculated values of $\langle M\rangle$. Contrary to the average magnetic moment, the local magnetic moments in the center (M_0) and on the surface (M_i) of the clusters were shown to be sensitive to the changes of the interatomic distance and of the interaction parameters. It is important to emphasize that the contributions of the *sp*-electrons to the total magnetic moments are missing. Typically, the *sp*-electrons have small magnetic moments which oppose those of *d*-electrons, and the overall magnetization is reduced. Nevertheless, the calculations reported in this work demonstrate that satisfactory results for the magnetic properties of transition metal clusters can be also obtained with a pure *d*-band Hubbard Hamiltonian.

These studies are complementary to the existing *ab-initio* calculations, as we have concentrated here rather on qualitative trends than on accurate description of particular systems. The main advantage of the considered tight binding model is its simplicity which allowed us to get a physical insight into the nature of the magnetic states of 4*d* transition metal clusters and reveal the microscopic reasons of their stability.

It is a pleasure to thank Dr. C. Lacroix for very illuminating discussions. Two of us (RGL and AMO) would like to acknowledge the hospitality of the Service de Recherche sur les Surfaces et l'Irradiation de la Matière of Centre d'Études de Saclay where part of the calculation has been made. We also acknowledge the financial support by CONACyT, Mexico (RGL), and by the Committee for Scientific Research (KBN) of Poland, Project No. 2 P03B 175 14 (AMO).

References

1. H. Tasaki, Phys. Rev. Lett. **69**, 1608 (1992); *ibid.* **75**, 4678 (1995); A. Mielke, Phys. Lett. A **174**, 443 (1993).
2. J.E. Hirsch, Phys. Rev. B **40**, 2354 (1989); J.C. Amandon, J.E. Hirsch, Phys. Rev. B **54**, 6364 (1996).
3. M. Kollar, R. Strack, D. Vollhardt, Phys. Rev. B **53**, 9225 (1996); D. Vollhardt, N. Blümer, K. Held, M. Kollar, J. Schlipf, M. Ulmke, Z. Phys. B **103**, 283 (1997).
4. G.M. Pastor, J. Dorantes-Dávila, K.H. Bennemann, Phys. Rev. B **40**, 7642 (1989).
5. G.M. Pastor, R. Hirsch, B. Mühlschlegel, Phys. Rev. Lett. **72**, 3879 (1994); Phys. Rev. B **53**, 10 382 (1996).
6. A.M. Oleś, Phys. Rev. B **28**, 327 (1983).
7. B.V. Reddy, S.N. Khanna, B.I. Dunlap, Phys. Rev. Lett. **70**, 3323 (1993).
8. A.J. Cox, J.G. Louderback, L.A. Bloomfield, Phys. Rev. Lett. **71**, 923 (1993).
9. A.J. Cox, J.G. Louderback, S.E. Apsel, L.A. Bloomfield, Phys. Rev. B **49**, 12 295 (1994).
10. L. Goodwin, D.R. Salahub, Phys. Rev. A **47**, R774 (1993).
11. J. Zhao, X. Chen, Q. Sun, G. Wang, Europhys. Lett. **32**, 113 (1995).
12. D. Kaiming, Y. Jinlong, X. Chuanyun, W. Kelin, Phys. Rev. B **54**, 11907 (1996).
13. G.W. Zhang, Y.P. Feng, C.K. Ong, Phys. Rev. B **54**, 17 208 (1996).
14. B. Piveteau, M.C. Desjonquères, A.M. Oleś, D. Spanjaard, Phys. Rev. B **53**, 9251 (1996).
15. J.S. Griffith, *The Theory of Transition-Metal Ions* (Cambridge University Press, 1961).
16. V.I. Anisimov, J. Zaanen, O.K. Andersen, Phys. Rev. B **44**, 943 (1991).
17. J.C. Slater, G.F. Koster, Phys. Rev. **94**, 1498 (1954).
18. D. Spanjaard, M.C. Desjonquères, Phys. Rev. B **30**, 4822 (1984).
19. J.R. Smith, J. Ferrante, J.H. Rose, Phys. Rev. B **25**, 1419 (1982).
20. D. van der Marel, G.A. Sawatzky, Phys. Rev. B **37**, 10 674 (1988).
21. K. Ohno, Theor. Chim. Acta **3**, 219 (1964); G. Klopman, J. Am. Chem. Soc. **86**, 4550 (1964).
22. C.D. Gelatt, Jr., M. Ehrenreich, R.E. Watson, Phys. Rev. B **15**, 1613 (1977).
23. M.C. Desjonquères, D. Spanjaard, *Concepts in Surface Physics*, 2nd Ed. (Springer, Germany, 1996).
24. Q. Sun, X.G. Gong, Q.Q. Zheng, D.H. Sun, G.H. Wang, Phys. Rev. B **54**, 10 896 (1996).
25. A.M. Oleś, G. Stollhoff, Phys. Rev. B **29**, 314 (1984).